Journal of Analytical and Applied Pyrolysis xxx (xxxx) xxx–xxx

Contents lists available at ScienceDirect

Journal of Analytical and Applied Pyrolysis

journal homepage: www.elsevier.com/locate/jaap

Heterogeneous kinetics of timber charring at the microscale

Franz Richter, Guillermo Rein*

Department of Mechanical Engineering, Imperial College London, London, SW7 2AZ, UK

ARTICLE INFO

Keywords:
Timber
Kinetics
Biomass
Fire
Pyrolysis
Charring

ABSTRACT

Timber is becoming a popular construction material even for high-rise buildings despite its poorly understood fire behaviour. In a fire, timber—a natural polymer—degrades in the thermochemical process of charring, causing it to lose structural strength. In spite of significant research on the physics of charring, the chemical kinetics—reactions and kinetic parameters for pyrolysis and oxidation—remains a scientific challenge to model accurately. Current kinetic models are either computationally too expensive or neglect key chemical pathways. Here we derive a new appropriate kinetic model for fire science at the microscale using a novel methodology. First, we built a kinetic model for each component of timber (cellulose, hemicellulose, and lignin) from literature studies and experiments of the components. Then, we combined these three models into one kinetic model (8 reactions, 8 chemical species) for timber. This approach accounts for chemical differences among timber species. However, the timber model is only able to reproduce the trend in the experiments when literature parameters are used. Using multi-objective inverse modelling, we extract a new set of optimised kinetic parameters from 16 high-quality experiments from the literature. The novel optimised kinetic model is able to reproduce these 16 and a further 64 (blind predictions) experiments nearly within the experimental uncertainty, spanning different heating rates (1–60 K/min), oxygen concentrations (0–60 %), and even isothermal experiments (220–300 °C). Furthermore, the model outperforms current kinetic models for fire science in accuracy across a wide range of conditions without an increase in complexity. Incorporated into a model of heat and mass transfer, this new and optmised kinetic model could improve the understanding of timber burning and has the potenial to lead to safer designs of timber buildings.

1. Introduction

Timber could become this century's construction material for high-rise buildings, because timber structures are strong, sustainable, and fast to construct. They are, however, flammable and present new challenges in terms of fire safety [1]. Most countries limit the height of timber buildings to 8 stories until the safety of taller structures can be demonstrated. Only a fundamental knowledge of timber's burning behaviour will allow us to demonstrate the safety of such structures. Fundamentally, the stability of a timber structure is controlled by the strength decay of timber, which is calculated from the charring rate of the timber. The dynamics—heterogeneous kinetics, heat transfer, and mass transfer—of charring, therefore, control the resistance and strength decay of timber in a fire. It is crucial to accurately capture both transport and heterogeneous kinetics, as both control the burning behaviour of timber [2].

The current literature is rich in kinetic models of the pyrolysis of timber for various applications of different complexity [3,4]. Oxidation reactions have been assumed negligible in all these studies. Recently, there has been growing evidence that these missing char and fuel oxidation reactions cause discrepancies in the predicted burning rate of timber in cone-calorimeter experiments (mesoscale) [5,6]. These findings suggest that a pure pyrolysis model—with no oxidation kinetics—is unsuitable for predicting charring, creating the need for heterogeneous kinetic models. A heterogeneous kinetic model includes both pyrolysis (reactions unaffected by oxygen) and oxidation (reactions affected by oxygen) reactions.

Only four main heterogeneous kinetic models exist [6–9], with none of them appropriate to predict the rate of burning and charring of timber. The model by Ranzi et al. [9,10] to calculate bio-oil production is currently too computationally expensive (32 reactions, 50 species). The model by Richter et al. misses the fuel oxidation pathway (key chemical pathway), which causes discrepancies at the mesoscale (g-samples) [6]. It is representative for pyrolysis models with an added char oxidation. Anca-Couce et al. [7] and Rein et al. [8] included char and fuel oxidation in their kinetic model, but consider only a single pyrolysis reaction for the fuel or each fuel component respectively, which is insufficient to explain the variable char yield and heat of

* Corresponding author.
E-mail address: g.rein@imperial.ac.uk (G. Rein).

https://doi.org/10.1016/j.jaap.2018.11.019
Received 13 August 2018; Received in revised form 12 November 2018; Accepted 14 November 2018

reaction observed for timber [4]. Failing to predict these two quantities would lead to inaccurate predictions of heat release and heat transfer at the mesoscale, which in turn would lead to an inaccurate predictions of the rate of charring.

In this study, we aim to build the first appropriate heterogeneous kinetic model for fire science, as no kinetic model of appropriate complexity for fire science exist. We will first show the relevance of kinetics measured at the microscale (mg-samples) to charring. Then we will outline our novel methodology of building a kinetic model at the microscale (mg-samples) including the selection of experiments, the development of an reaction scheme, and the value of kinetic parameters. Afterwards, we will analyse and discuss the validity of our methodology, our predictions of variable char yield and heat of reaction, and our model results. The latter section also includes a comparison of our novel model with kinetic models from the literature. In the last section we will summarise and conclude our findings.

2. Relevance of kinetics measured at the microscale (mg-samples) to charring

In fire science, it is conventionally assumed that the temperature at which timber turns into char, at an infinitely thin reaction zone, is the pyrolysis temperature [11]. The assumption is that heat transfer (physics) limits charring, thus eliminating the need for research on degradation kinetics of timber for charring. This is not necessarily true. Furthermore, the use of thermogravimetric analyser (TGA) data to determine the kinetics of timber has also been questioned, due to insufficient evidence that the conditions in an analyser match those in a fire [12]. The above imply that kinetics and TGA are irrelevant for research on the charring and burning rate of timber. In this section, we will argue that kinetics and TGA are relevant to charring of timber.

In 1983, Atreya inferred that there are two pyrolysis regimes [2]: the first controlled by kinetics, the second controlled by heat diffusion. The first regime represents the development of a pyrolysis zone (a reaction zone of finite size) and the second regime the propagation of this zone. Atreya suggested that his observations could be tested using the Damkoehler number, which compares the characteristic timescale of heat diffusion and chemical kinetics. The ratio of these two timescales tells us if either of the two process (heat diffusion or chemical kinetics) is limiting the pyrolysis process and controls the rate of charring. Here, we will use that approach to test the application of the pyrolysis temperature to charring.

Let us consider a timber beam in a fire as a thermally thick slab with one boundary (x = 0) exposed to a fire, as shown in Fig. 1a. We use the Damkoehler number ($Da = \eta\delta^2/\alpha$) to compare the timescales of heat transfer and kinetics, where α is the thermal diffusivity of char, δ the char depth, and η the rate constant. Using typical kinetic [13] and transport [14] timescales reveals that both chemistry and diffusion control charring (Fig. 1b) in three different regimes. In the onset regime the material is heated as if it is inert. Heat transfer (diffusion) to and within the timber limits the degradation (onset region) and temperatures are too low for chemical reactions to take place, therefore the Damkoehler number is invalid in this regime. Once sufficiently high temperatures are reached, a pyrolysis zone (thin char layer) develops, whose growth is limited by chemistry. Heat transfer (diffusion across the char layer) is limiting again once a thick char layer is formed and the pyrolysis zone propagates within the timber. Mass diffusion is faster than heat diffusion [16], meaning that the same analysis holds for mass transfer. A model of charring, therefore, needs to incorporate heat transfer, mass transfer, and kinetics.

In the literature, kinetics are traditionally measured using the residual mass and temperature histories of mg-samples from a small furnace (microscale experiments). This furnace is called a thermogravimetric analyser (TGA) and the samples are assumed sufficiently small for heat and mass transfer to be negligible. The sample is heated at a constant rate (β) below 100 K/min, but the appropriateness of these

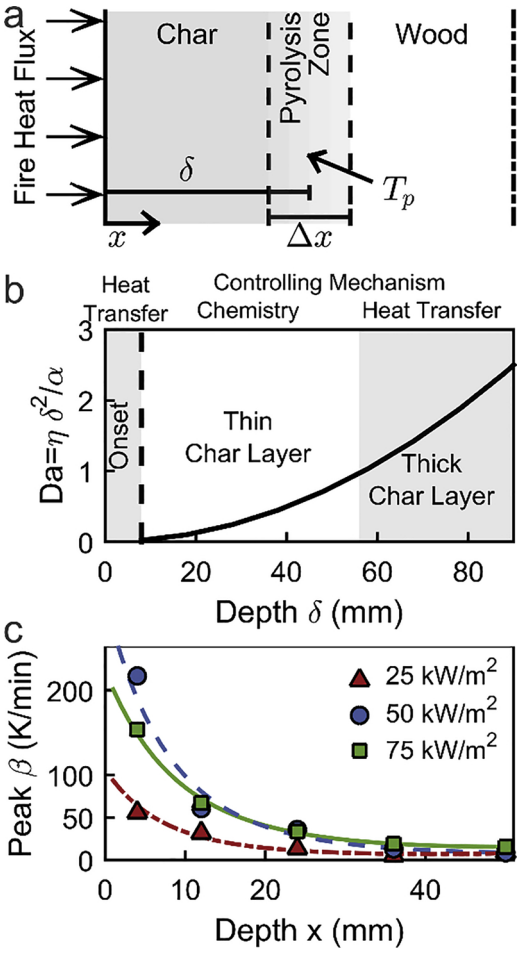

Fig. 1. (a) Diagram of a timber slab exposed to fire, with charring modelled as a moving front and length scales for the analysis in b. and c. (b) Evolution of Da with char depth, with parameters $\eta = 2.82 \cdot 10^{-4} s^{-1}$ [13] and $\alpha = 0.916\, mm^2/s$ [14]. The onset regime is displayed at an arbitrary size for clarity, and is actually smaller than displayed. (c) Peak heating rate at each depth for each heat flux from the experiments in [15].

conditions for fire science is still debated. Spearpoint and Quintiere [15] studied the burning of timber in a cone calorimeter under heat fluxes similar to those in a real fire and reported in-depth temperatures. We calculated heating rates from these temperature-time profiles by fitting polynomials to the data at each depth and heat flux, and differentiating the polynomials. This approach revealed a decay of the maximum heating rate with depth. Fig. 1c shows that below a depth of 10 mm (x > 10 mm), the heating rate is always within the range of a TGA (β < 100 K/min). This analysis proves that kinetics measured at the microscale in a TGA are relevant for predicting the charring rate of timber.

3. Methods

3.1. Methodology

Deriving a reaction scheme and kinetic parameters from ones own experiments is common in fire science [7,17–19]. This minimises the uncertainty due to differences in species, apparatus, and procedure between experiments. At the same time, it restricts the size of the dataset (< 12 experiments usually), which could give rise to a compensation effect in a complex kinetic model (> 2 reactions) [20]. The compensation effect means that one parameter deviates from its correct value to compensate for either another incorrect parameter or a deficit

in the model.

The studies of Ranzi et al. [10], Miller and Bellan [3], and Anca-Couce and Obernberger [21] instead used data from the literature to build their kinetic models. These models are based on databases with several species and result in good agreement with a large number of experiments (> 12 experiments). The success of the Ranzi and Bellan model suggests a greater robustness of this approach. Each of these three studies assumed that the three main components (cellulose, hemicellulose, and lignin) of timber degrade independently. A kinetic model was derived for each component using literature studies of both the individual component and timber as a whole. Following this assumption one should be able to study the three components in isolation and build a kinetic model of timber based on their liner superposition.

Here, we first build a kinetic model using only studies on the individual components of timber. No experiments or studies of timber as a whole were used at this stage. Great care was taken to quantify the error of each experiment and to choose only the ones with the lowest error. Only in the second stage, we evaluated a subset of kinetic parameters using experiments of timber from the literature (as explained in section 4.2). To the best of our knowledge, no other study has followed this methodology to test whether a heterogeneous kinetic model for the charring of timber can be derived solely from studies of its three components.

3.2. Experiments from the literature

Reliable experiments were selected by defining a criteria for the maximum sample mass and heating rate below which transport limitations are negligible. For cellulose, we used the conditions defined in [22]. For biomass in an inert atmosphere, Stenseng et al. showed that the sample mass should be below 10 mg and β below 40 K/min [23]. In an oxidative environment, other investigators [7,24] showed that either the sample mass should be below 2 mg or the height of the sample layer should be below 120 μm. We applied the same criteria as for biomass to hemicellulose and lignin.

We then created a database of experiments from the literature (supplementary material Table S1) spanning the whole range of expected conditions in a fire that are accurately measurable in a TGA. The experiments include both isothermal (constant furnace temperature) and non-isothermal (constant heating rate) conditions. Cellulose was studied from 1 to 65 K/min [25,26], 250–286 °C [27] and up to 21% O_2 [28]. Hemicellulose was studied from 3 to 20 K/min [29] and up to 60% O_2 [18]. Lignin was studied from 2 to 30 K/min [30], 226–435 °C [31], and up to 60% O_2 [19]. A range of timber species were studied from 2.5 to 60 K/min [7,32,33], 220–300 °C [34], and up to 21% O_2 [7,24,35,36]. In total, 80 experiments were used.

3.3. Kinetic model

Each reaction in the kinetic model is assumed to be of the following form, Eq. 1.

$$B + \nu_o O_2 \rightarrow \nu C + (1-\nu)V \tag{1}$$

Where B represents the solid-phase reactant, C the solid-phase product, and V the released volatiles. ν_o represents the amount of consumed oxygen—not evaluated here as oxygen assumed to be present in excess—and ν is the solid yield. The formulation of the rate of reaction of multiple solid-phase reactants has been outlined previously for cellulose [22], and is simplified here to one solid-phase reactant, but extended to other components, in Eq. 2.

$$\dot{\omega} = \eta m_s^n y_{O_2}^{n_o} \tag{2}$$

Where $\dot{\omega}$ is the rate of reaction, η the rate constant according to Arrhenius $\eta = Aexp\left(-\frac{E}{RT}\right)$, n the reaction order of the k th species, y_{O_2} the volume oxygen fraction, and n_o the order of oxidation (0 for pyrolysis). m_s is the mass of the reacting species normalised to its source species, see [37]. The mass fractions of the source species—cellulose, hemicellulose, and lignin—are obtained from the composition of the sample. We denote the overall normalised sample mass ($m = \sum m_s$) by m, the pre-exponential factor by A, the universal gas constant by R, and the activation energy by E. The boundary and remaining initial conditions are defined in Eq. (3).

$$\left.\begin{array}{c} T(0) = T_0 \\ y_{O_2}(t) = y_{O_2}(0) \\ T(t) = \begin{cases} T_0 + \beta t \ if \ T < T_R \\ T_R \ if \ T \geq T_R \end{cases} \end{array}\right\} \tag{3}$$

Where T is the surface temperature of the sample, T_0 the initial surface temperature, T_R the peak reactor temperature and β the heating rate.

3.4. Optimisation

We used multi-objective optimisation to re-evaluate (inverse model) kinetic parameters, as outlined in [22], within a range based on the literature. The code AMALGAM [38] was used for the multi-objective optimisation. All optimisations converged after roughly 10^4 function evaluations. Eqs. (4) and (5) present the objective function for non-isothermal and isothermal experiments respectively. Compared to [22], the scaling was modified to include experimental uncertainties.

$$\phi_i = \left(\frac{1}{N_1} \sum\nolimits_{N_1} \left(\frac{m_e - m_p}{\sigma_{m_e}} \right)^2 + \frac{1}{N_2} \sum\nolimits_{N_2} \left(\frac{\dot{m}_e - \dot{m}_p}{\sigma_{\dot{m}_e}} \right)^2 \right) \tag{4}$$

$$\phi_i = \frac{1}{N_1} \sum\nolimits_{N_1} \left(\frac{m_e - m_p}{\sigma_{m_e}} \right)^2 \tag{5}$$

Where ϕ is the error, N the number of data points, m the sample mass, $\dot{m}$ the mass loss rate, and σ the experimental uncertainty. The subscripts e and p refer to experimental and predicted respectively. The number of points (N) was determined by the experimental data points available.

4. Results

4.1. Development of the reaction scheme

Both model and parameter uncertainties were used to determine the appropiate complexity of the reaction scheme. We minimised the model uncertainty—uncertainty from missing chemical paths—by requiring that the reaction scheme explains four key experimental observations: diminishing char yield at high heating rate, accelerated mass loss in air, char yield dependent heat of reaction, and presence of an intermediate species [4]. We assessed these observations as well-established and most relevant to charring, based on our review of the literature. We minimised the parameter uncertainty—uncertainty in the kinetic parameters—using predictions of experiments excluded from the derivation (blind predictions).

The Broido-Shafizadeh mechanism (Fig. 2a) with the parameters from [13] was used to model the pyrolysis of cellulose. This combination performs well in a-priori predictions and shows optimal complexity for fire science [22]. It explains the diminishing char yield at high heating rates, the presence of an intermediate species, and the char yield dependent heat of reaction observed for both cellulose and timber [4]. The role of oxygen in the degradation was modelled by introducing a fuel oxidation reaction as a competing reaction to fuel pyrolysis (Ohlemiller's approach) [7]. We assume that oxygen interacts with both cellulose and active cellulose in the same way, as they only differ in their degree of polymerization [13]. We, therefore, used two fuel oxidation reactions (Fig. 2), one from cellulose (R4a) and one from active cellulose (R4b), which produced char with the same kinetic parameters [28]. Therefore, these reactions are reported henceforth as one reaction R4.

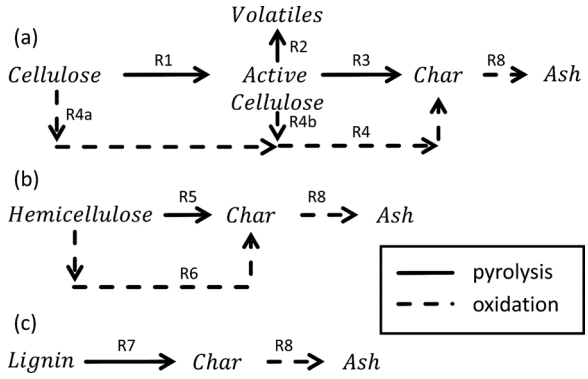

Fig. 2. Proposed reaction scheme for timber. Reactions R3-R8 yield the shown solids as well as volatiles.

The mass loss rate of hemicellulose from timber resembles a one-step pyrolysis reaction (Fig. 2b) [29]. With the kinetic parameters by Ramiah [39], the predictions match the experiment closely [29],with an average error (φ) of 1.1 times the experimental uncertainty σ_e ($\varphi = 1.1\sigma_e$). The influence of oxygen was modelled with a competing fuel oxidation. Due to the lack of alternative kinetic parameters that could satisfactorily reproduce the experiments in [18], we chose parameters from timber [7] and estimated a char yield of 40% from [18] for the fuel oxidation. Notably, this char yield is abnormally high as will be revealed later by our re-evaluation.

For lignin, the reaction scheme and parameters from Manya et al. [40] (Fig. 2c) show good agreement with the experiments ($\varphi = 1.6\sigma_e$) [30]. In contrast to cellulose, oxygen hinders the mass loss of lignin [19]. A preliminary study revealed that the Ohlemiller scheme is unable to capture this effect. The main discrepancy arises from the difference in char reactivity between chars from lignin, cellulose, hemicellulose and timber. We judge this small discrepancy as acceptable compared to the required complexity to eliminate it.

Other organic components (extractives) were added to hemicellulose [3]. The detailed product composition of pyrolysis varies by less than 10% with ash content [41]. The influence of ash is, therefore, negligible and not modelled. All reaction pathways are assumed to produce the same char. The char oxidises through a reaction with the parameters from [28], which shows good agreement with experiments ($\varphi = \sigma_e$) [7].

The resultant reaction scheme and kinetic parameters referred to as KP I are all taken from the literature and shown in Fig. 2.

4.2. Value of the kinetic parameters

The experimental data in Fig. 3–5 reveal three trends: the peak rate of reaction $\dot{\omega}_m$ and corresponding temperature T_m increase with heating rate (Fig. 3 & 5), oxygen accelerates the mass loss with $\dot{\omega}_m$ increasing (Fig. 5 & S1) and T_m decreasing (Fig. 4 left), and the char yield diminishes with isothermal temperature (Fig. 4 right). An accurate kinetic model should reproduce all these trends within their experimental uncertainty. The reaction scheme with the first set of kinetic parameters KP I—labelled with I in Fig. 3–5—reproduces nearly all these trend, but not within the experimental uncertainty. The model (KP I) underpredicts T_m under sub-atmospheric $[O_2]$ (see Fig. 4), overpredicts $\dot{\omega}_m$ as $[O_2] \to 0$ (see Fig. 3), and underpredicts $\dot{\omega}_m$ as $[O_2] \to 0.21$ (see Fig. 3). Depending on the heating rate this switch occurs around 5–10 % O_2. Furthermore, the model predicts that $\dot{\omega}_m$ will decrease with oxygen concentration $[O_2]$ rather than increase (Fig. S1). These major discrepancies can be eliminated by re-evaluating a subset of the kinetic parameters using inverse modelling.

The parameters of R5 to R7 were judged to be the most uncertain, because of the few available fundamental studies and first-principle calculations in the literature. Hence, we first recalculated the parameters (activation energy, pre-exponential factor, reaction order, oxidation order, yield) of reaction R5 to R7 from experiments of hemicellulose and lignin [18,19,29–31], which only slightly improved the predictions of timber. As the predictions were the worst in the region of hemicellulose and cellulose degradation, we used inverse modelling to find the kinetic parameters of cellulose and hemicellulose from experiments of timber. Different types of cellulose decompose at different temperatures [26], due to differences in their crystal structure or size [42]. We followed Mamleev et al. [42] and accounted for the difference in crystallinity by adjusting the pre-exponential factor of R2 and R3 by the same factor (0.37). Together with R5 (all kinetic parameters), we obtained this factor through inverse modelling from the pyrolysis experiments of [7,34]. We then calculated the parameters of R4 and R6 (all parameters) from experiments in an oxidative environment [7], and kept R7 from our optimisation to lignin experiments [30]. The final kinetic model (KP II) was, therefore, optimised to [7,30,34], while predictions of all other experiments are blind. All parameters were optimised within a range based on the literature.

The new set of kinetic parameters (KP II given in Table 1 with KP I) reproduces all observed trends nearly within the experimental uncertainty, as shown in Fig. 3–5. Fig. 6 shows the 12 optimised and 49 blind predictions of non-isothermal experiments including different species and heating rates. They are nearly all within reasonable accuracy (± 25%).

5. Discussion of the methodology

In the previous section we found that a kinetic scheme consisting of individually evaluated kinetic parameters was unable to correctly predict the residual mass-temperature histories of timber. This finding also holds in gas-phase kinetics [43]. For gas-phase kinetics, one proposed

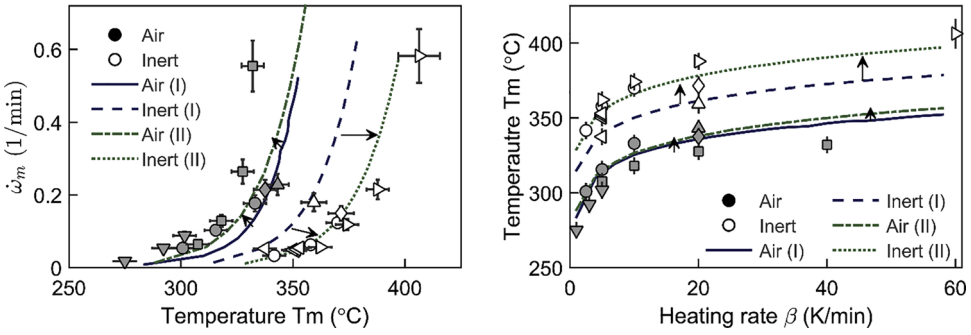

Fig. 3. Left: Comparison of experimental and predicted $\dot{\omega}_m$ against corresponding temperature T_m of non-isothermal experiments in air and inert atmosphere. Right: Predicted and experimental T_m against β of non-isothermal experiments in air and inert atmosphere. The experiments are by Anca-Couce et al. (dots) [7], Branca and Di Blasi (squares) [24], Liu et al. (triangle up) [36], Su et al. (diamond) [35], Kashiwagi and Nambu (triangle down) [28], Ding et al. (triangle right) [32], and Gronli et al. (triangle left) [33].

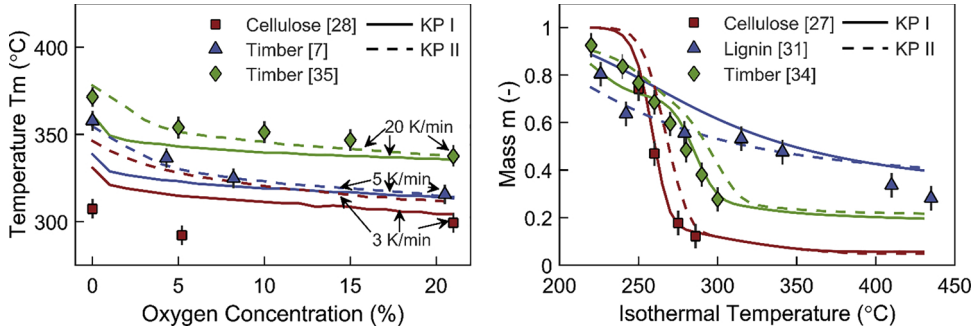

Fig. 4. Left: Shift of T_m to lower temperatures with $[O_2]$ in non-isothermal experiments. Right: Predicted and experimental final yield of the isothermal experiments of cellulose, lignin, and timber.

method is to recalibrate the individual rate constant within their uncertainty to the final fuel to account for interactions between components and respective uncertainties of rate constants. Here, we followed the same methodology by first deriving rate constants for each timber component and then recalibrating these to a subset of the timber experiments. This recalibration accounts for: (1) interaction between components, (2) deficit knowledge of chemical pathways, and (3) insufficient accuracy of the kinetic parameters. The latter two are the most likely sources of uncertainty, as Raveendran et al [44] were able to reproduce the TGA measurements of timber with TGA measurements of the extracted components of timber. Hence, the effect of interactions (uncertainty (1)) on the mass-temperature histories is likely insignificant.

Frenklach [45] hypothesised that the past success of research in gas-phase kinetics stems from the community's approach to derive practical reaction mechanisms from detailed reaction mechanisms, instead of trying to slowly build up complexity. That approach minimises uncertainty from deficit knowledge of chemical pathways (uncertainty (2)). The study of detailed reaction mechanisms for pyrolysis of biomass is still in its infancy [46], and detailed mechanisms of combined pyrolysis and oxidation are none-existant. Our approach was, therefore, to build a simple reaction scheme based on well-established knowledge and to minimise model uncertainty (missing chemical pathways) through the use of experimental observations.

The incomplete knowledge of chemical pathways and the significant uncertainty in TGA experiments leads to a large uncertainty in kinetic parameters (uncertainty (3)), which we found previously for cellulose by comparing the optimal parameters for isothermal and non-isothermal experiments [22]. Here, we found that the optimal kinetic parameters for degradation reactions of timber and of its components differ. For example, in Fig. 7 we optimised the pre-exponential factors of R2 and R3 to the experiments of timber and cellulose simultaneously. The appearance of a Pareto front represents a set of non-dominant solutions. The optimal solution for R2 in timber differs to the optimal solution of R2 for avicel cellulose. This difference in the pyrolysis of different celluloses has previously been reported by [26,44], but it extends to all other components (Fig. 7). We attribute these differences between wood and its components to the difference in chemical structure (and behaviour) of the components obtained from wood and those obtained commercially. Raveendran et al. [44] found that the superposition approach only works if cellulose extracted from wood, and not commercial cellulose, is used. It is, therefore, unlikely that the Pareto fronts stem from interaction between cellulose, hemicellulose, and lignin within wood. We can infer that one can only use commercial surrogates of the components of timber to study their lumped reaction schemes. Rate constants, however, still have to be evaluated from experiments of timber, meaning that our methodology is valid.

6. Discussion of variable char yield and heat of reaction

The definition of char yield depends on the apparatus. For example, in a TGA ($\beta < 100\,K/min$) the residual mass asymptotically approaches a constant value above a set temperature. This value is taken as the char yield. TGA experiments are terminated below 1000 K. On the other hand, in a drop tube furnace ($\beta \gg 100\,K/min$) the particle is rapidly heated to the furnace temperature and then held at that temperature for a couple of second. The char yield is the residual mass of the particle after exiting the furnace. Drop tube furnace experiments are terminated above 1000 K. To obtain the char yield over a wide range of heating rates, we have to join these two measurements.

We join these measurements by defining the char yield as the residual mass obtained in an experiment as $t \to \infty$. The difference in the final reactor temperature at low (TGA) and high (drop tube) heating rates was accounted for by assuming all apparatuses reached a temperature of 1673 K (maximum recorded). In the simulations, the sample was then held at that final furnace temperature for 5 min, which represents $t = \infty$. Transient effects were found at shorter times. All measurements and predictions in Fig. 8 are assumed to comply with this

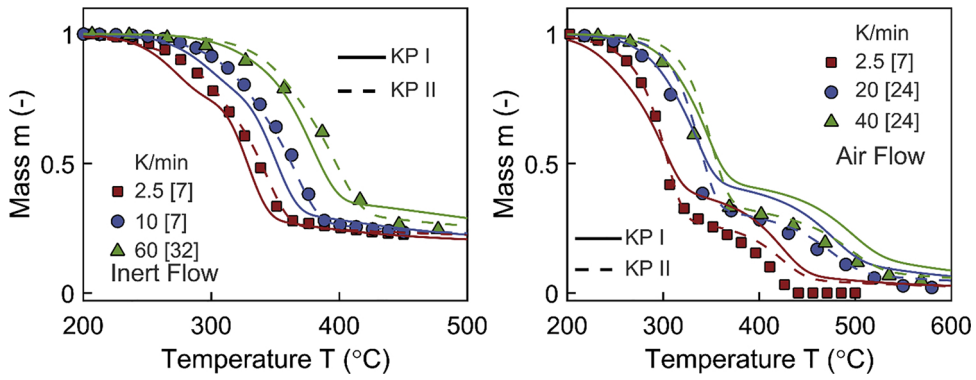

Fig. 5. Prediction of experiments in inert (left) and oxidative (right) environment at several heating rates.

Table 1
Overview of the two sets of kinetic parameters for each reaction, with uncertainties for calculated values. The reaction scheme for both sets of kinetic parameters (KP I and KP II) is the same. The pre-exponential factor of R2 and R3 were adjusted by the same value, to represent the difference between pure cellulose and cellulose in timber. Values without uncertainties are taken from the literature. Uncertainties below 0.001 are reported as 0. The uncertainty reported for each of the kinetic parameters represents the standard deviation found at the Pareto front. For reaction R2, R3, R5 and R7 the two objectives are the isothermal and non-isothermal experiments, while for R4 and R6 the two objectives are the sub-atmospheric and atmospheric experiments.

	KP	R1	R2	R3	R4	R5	R6	R7	R8
E	I	243	198	153	160	125.5	75	65.4	160
(kJ/mol)	II	243	198	153	179 ± 13	166 ± 16	96 ± 29	72 ± 6.8	160
log A	I	19.5	14.5	10.1	12.4	9.34	5.66	2.61	9.75
(log s^{-1})	II	19.5	14.1 ± 0.03	9.69 ± 0.03	14.2 ± 1.2	12.5 ± 1.6	7 ± 3.5	4 ± 0.68	9.75
n	I	1	1	1	1.3	1	1	3	1
(-)	II	1	1	1	1 ± 0.16	1 ± 0.1	0.5	4 ± 0	1
n_{O_2}	I	0	0	0	0.5	0	0.5 ± 1.7	0	0.78
(-)	II	0	0	0	1 ± 0.35	0	2 ± 0.7	0	0.78
ν	I	1	0	0.35	0.21	0.21	0.4	0.3	0.03
(-)	II	1	0	0.35	0.13 ± 0.04	0.29 ± 0.05	0.1 ± 0.001	0.33 ± 0.01	0.03

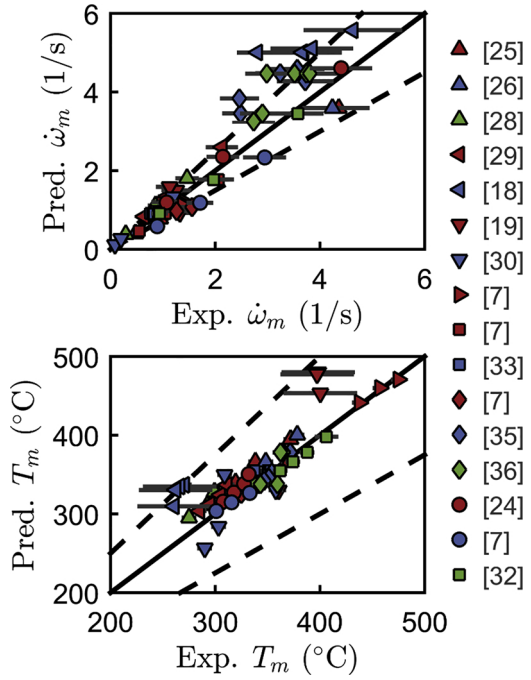

Fig. 6. Comparison between prediction and experiments of $\dot{\omega}_m$ and T_m for all non-isothermal experiments. The dashed line represent ± 25%.

definition.

Fig. 8 compares the predicted and measured char yield from 2.5 K/min to 720,000 K/min. Both the predictions and experiments show that char yield reduces asymptotically to constant value at high temperatures. The model, however, predicts this value to be 0.16 while measurements put this value at 0.02. In the model, a value of 0.16 represents that all cellulose was converted to volatiles, and that char was only formed by hemicellulose and lignin. The measurements suggest that wood as a whole can be converted to volatiles, leaving behind only inorganic matter (around 3% [7]). Hence, a more accurate description of the kinetics should include competative reactions for hemicellulose and lignin. However, as shown in Section 2, the heating rates in charring are low ($\beta < 100\,K/min$) for which our model slightly under predicts the measurements. This under prediction is expected as TGA measurements are commonly terminated before 1000 K and not held at high temperatures. The lower final temperature and shorter experimental time in the experiments compared with the simulations lead to higher residual mass, as the residual mass is a combination of char and partially degraded wood. Hence, we believe our model captures this key chemical phenomenon (a reduction in char yield) accurately within the range of interest ($\beta < 100\,K/min$).

The second limitation of previous heterogeneous kinetic models was their inability to predict the variable heat of pyrolysis with char yield. Fig. 9 compares the measurements of the heat of pyrolysis of spruce with two predictions. Prediction A used the heat of pyrolysis for cellulose from [47] and for hemicellulose and lignin from [7]. As shown in Fig. 9, prediction A captures the trend of the heat of pyrolysis with char yield but not within the experimental uncertainty. If we adjust the heat of reaction of R3 from −1 MJ/kg (Pred. A) [47] to -3.8 MJ/kg (Pred. B) [48], we capture the measurements within their uncertainty. Hence, our model is able to capture this key chemical phenomenon (a reduction in the heat of reaction) accurately using an optimised value for the heat of reaction.

Models from the literature that included fuel oxidation reactions failed to include competing pyrolysis reactions, meaning the char yield and heat of pyrolysis were constant. For example, when we derived the char yield (as $t \to \infty$) from such a model (three parallel reaction) with a predefined char yield, call model L here), we found a constant value (see supplementary material Figure S2). As the char yield is constant with heating rate and isothermal temperature (see Supplementary material) we cannot plot the variation of heat of pyrolysis against char yield. Consequently, if a kinetic model fails to predict a variable char yield it also fails to predict a variable heat of pyrolysis.

Notable, the previous discussion focussed only on the heats of reaction (heat of pyrolysis) in the absence of oxygen. Anca-Couce et al. [7] showed that the heats of reaction in the presence of oxygen can be predicted accurately when using competing pyrolysis and oxidation reactions. Our model—that includes competing pyrolysis and oxidation reactions—should therefore be able to capture the heat of reaction in the presence of oxygen.

7. Discussion of the results

Our derived reaction scheme with parameters from the literature (KP I) predicts the experiments of timber, but not within the experimental uncertainty. After inverse modelling using half of the parameters, the predictions match all experiments closely, see KP II in Fig. 10. The obtained parameters (Table 1) are within the range reported in literature [4]. For example, the activation energy R5 is within 4% of that reported for hemicellulose of timber (160 kJ/mol) [50]. The parameters for lignin agree well with Manya et al. (see KP I) and Dauenhauer et al (E = 74.42 kJ/mol, log A = 4.14 log s^{-1}) [51]. The activation energy and pre-exponential factor of R2 are within the

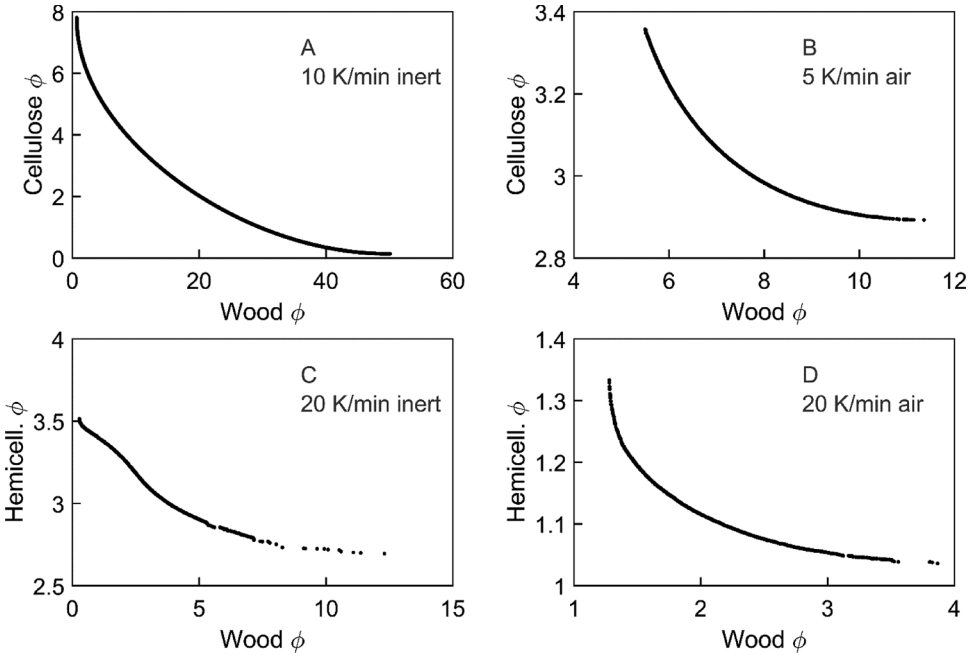

Fig. 7. (A) Error from the multi-objective optimisation between cellulose [26] and timber [7] at 10 K/min in inert atmosphere. (B) Error from the multi-objective optimisation between cellulose [28] and timber [7] at 5 K/min in air. For the experiments of [28] only the measurement of the mass loss rate were available. These experiments were optimised only to the mass loss rate. (C) Error from the multi-objective optimisation between hemicellulose [18] and timber [35] at 20 K/min in inert. (D) Error from the multi-objective optimisation hemicellulose [18] and timber [35] at 20 K/min in air. The error is defined in Eq. (4). A value below one represents predictions within the experimental uncertainty, while a value above represents predictions outside the experimental uncertainty.

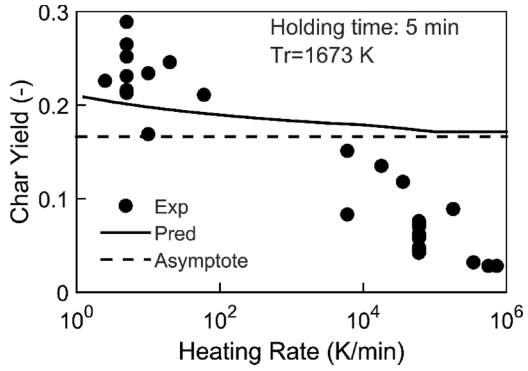

Fig. 8. Comparison between measured and predicted (model: KP II) char yield. The measurements are from [7,32,33,49]. All experiments and simulations are in inert atmosphere. Tr is the maximum furnace temperature, the holding time is the time the furnace is held at the maximum furnace temperature.

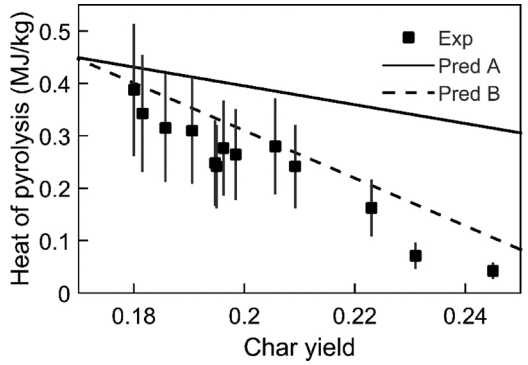

Fig. 9. Comparison between measurements [48] and predictions (KP II) of the heat of pyrolysis with the heat of reactions taken from [7,47] (Pred A) and from [7,48] (Pred B).The error is the lower bound error by [48] and could potentially be larger.

current theoretical limits (log A = 13–14 log s^{-1} E = 190–200 kJ/mol [22]). Furthermore, our optimisation found that the parameters (activation energy, pre-exponential factor, reaction order) of R4 are the same as R2, except for a lower activation energy. This difference in the activation energy of R2 and R4 between the two reactions is consistent with Mamleev et al. [42] proposal that oxygen only accelerates the release of volatiles.

Our kinetic model is compared here to the heterogeneous kinetic models by Richter et al. (10 reactions, 9 species) [6]—which is Bellan's pyrolysis model [3] with an added char oxidation reaction and called Bellan's hereforth—and by Ranzi (20 reactions, 19 species) [9,10] (see Supplementary material for necessary simplification). We choose these two models as they represents the current state-of-the-art for heterogeneous kinetic models.

Bellan's model predicts the experiments of cellulose and timber close to the experimental uncertainty (Fig. 10). Despite missing a fuel oxidation pathway, the predictions of Bellan's model are better in reactive environments than inert atmosphere. For example, the mean error for the experiments of Anca-Couce [7] reduces with increasing oxygen concentration from 1.9 in nitrogen to 1.4 in air to 1.1 in subatmospheric conditions. This agreement falsely suggests that fuel oxidation is unimportant, as the model by Bellan predicts a too low temperature of the peak mass loss rate in nitrogen. Comparing, the model to KPI and KPII one can conclude that it is outperformed by both. KPI shows a lower mean error in each experiments other than for cellulose and [7] ($[O_2] > 0$). KPII performs worse for cellulose and hemicellulose, but significantly outperforms the Bellan model for timber.

Similar observations are made for the Ranzi model, which performs similarly to KPI for timber but is outperformed by KPII (Fig. 10). Hence, one can conclude that our reaction scheme with KP II outperforms current heterogeneous kinetic models of similar and greater complexity. Notably, our heterogeneous model has been developed to predict solid yields of timber under various heating scenario and oxygen concentrations, and our conclusions only hold within that framework.

With this extensive agreement of the reaction scheme and KP II with experiments, literature, and theoretical calculations, we judge the kinetic model as valid and appropriate for fire science. Notably, our validation is significantly broader than previous ones for heterogeneous models in the number of experiments (80) and heating scenarios (isothermal vs non-isothermal). Results from Section 2 and the literature [37] suggest that a better performance at the microscale improves predictions at larger scales. In the upscaling, we assume that the effect of secondary reactions of volatiles are negligible for two reasons.

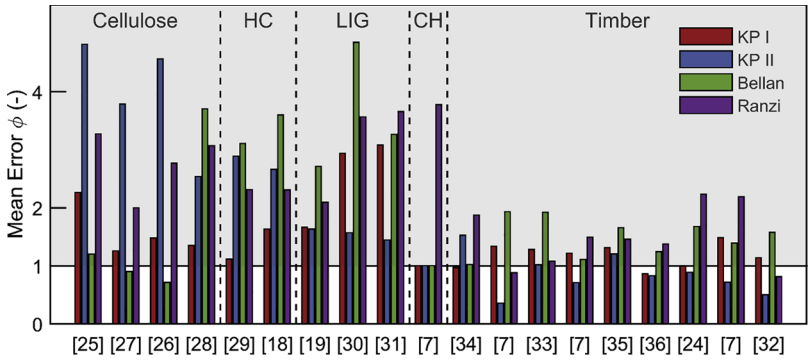

Fig. 10. Mean Error (Eqs. (4) and (5)) between each kinetic model and all experiments grouped by their respective studies. The mean error is normalised to the experimental uncertainty as defined in Eq. 4 & 5. A value below one represents predictions within the experimental uncertainty. The experiments of Anca-Couce [7] are split, in order, into: $[O_2] = 0$, $0 < [O_2] < 21$, $[O_2] = 21\%$. HC – Hemicellulose, LIG – Lignin, CH – Char.

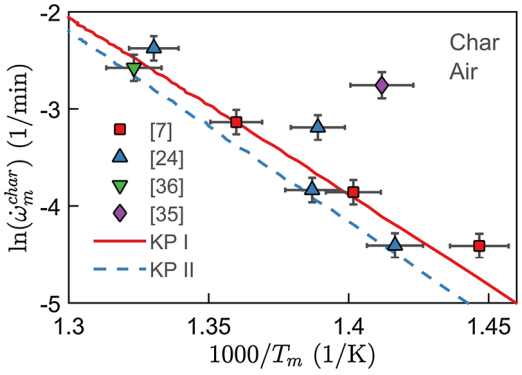

Fig. 11. Comparison between predicted and experimental peak rates of char oxidation in air.

Firstly, previous studies found good agreement of mesoscale (g-samples) predictions and experiments using kinetic models without secondary volatile reactions [3,37]. Secondly, following the approach of Bal and Rein [52] there are currently insufficient experiments of secondary reactions to justified the required increase in complexity to model secondary volatile reactions. Hence, given the current state of knowledge and experiments, it is justified to assume that our model captures the relevant chemical kinetics across scales. Incorporated into a mesoscale (benchscale) model, our kinetics should significantly improve the prediction and understanding of the burning of timber.

The main limitation of this study is the assumption of only one universal char species. Currently it is believed that fuel oxidation produces char with significantly different reactivity to pyrolysis char [8]. The role of oxygen, however, in thermal degradation is still unexplained [42]. For the sake of simplicity and because of the good agreement with experiments—within experimental uncertainty as shown in Fig. 11—the assumption of one char species was deemed reasonable.

8. Conclusion

This paper presents a novel heterogeneous kinetic model for the thermal degradation (charring) of timber, valid for different timber species, oxygen concentrations, and heating conditions. Predicting the charring of timber is essential to accurately predict the structural response of timber to fire. Opposite to the conventional assumption that chemistry is of minor importance, our dimensional analysis using the Damkoehler number proves that chemistry and heat transfer together limit charring. An accurate model of charring needs to incorporate both. An appropriate heterogeneous chemical kinetic model for fire science, however, was missing from the literature. We tested the hypothesis that such an appropriate heterogeneous kinetic model can be derived solely from literature studies of timber's three main components: cellulose, hemicellulose, and lignin. Treating each component in isolation resulted in an appropriate reaction scheme of 8 reactions and species for timber, but inappropriate kinetic parameters. The reaction scheme explains the observed trends in solid yields and heat of reaction of timber across different heating and oxygen conditions. The kinetic parameters (KP I) failed to capture the experiments, as the average error for microscale experiments of timber is 1.2 times the experimental uncertainty. Inverse modelling of half of the kinetic parameters to 16 experiments was required (producing KP II) to account for the interactions between the components, the deficit knowledge of chemical pathways, and the uncertainty of rate constants. Afterwards the kinetic model reproduces 80 high-quality literature experiments under fire conditions—on average 0.9 times the experimental uncertainty for timber—including different heating rates (1–60 K/min), oxygen concentrations (0–60 %), and isothermal temperatures (220–300 °C). This performance outperforms current state-of-the-art models by roughly 35% on average with respect to the literature model. Furthermore, our parameters compare well with the literature as the activation energy for hemicellulose is within 4% of the literature while for cellulose it lies in the theoretical calculated limits (190–200 kJ/mol). With this extensive agreement of our kinetic model with experiments, literature studies, and theoretical calculations, we judge the kinetic model as valid and appropriate for fire science. We believe that, if our kinetics were incorporated into a heat and mass transfer model, they would significantly improve the prediction and understanding of timber's burning behaviour.

Acknowledgment

This work was sponsored by the Engineering and Physical Sciences Research Council (EPSRC) (EP/M506345/1), Ove Arup, the SFPE Foundation Award, and the European Research Council (ERC) Consolidator Grant HAZE (682587). We would like to thank Professors Anca-Couce (TU Graz, Austria), Branca (C.N.R. Napoli, Italy), Ding (USTC, China), Garcia-Perez (WSU, USA) and Chow (Hong Kong Poly, China) for sharing their data with us and Professor Ek (KTH, Sweden) for sharing details of her study with us. We also thank the following people for their helpful comments and discussions: Professor Merci (UGhent, Belgium), Professor Atreya (UMich, USA), Dr Nils Rönner, Dr Francesco Restuccia, Dr Guoxiang Zhao, Yuqi Hu, Han Yuan, Eirik Christensen, and Matt Bonner (all from Imperial College London, UK).

Appendix A. Supplementary data

Supplementary material related to this article can be found, in the online version, at doi:https://doi.org/10.1016/j.jaap.2018.11.019.

References

[1] S. Deeny, R.M. Hadden, A. Lawrence, B. Lane, Fire safety design in modern timber buildings, Struct. Eng. 96 (1) (2018).
[2] A. Atreya, Pyrolysis, Ignition and Fire Spread on Horizontal Surfaces of Wood, Harvard University, 1983.

[3] R.S. Miller, J. Bellan, A generalized biomass pyrolysis model based on superimposed cellulose, hemicellulos eand liqnin kinetics, Combust. Sci. Technol. 126 (1997) 97–137, https://doi.org/10.1080/00102209708935670.

[4] A. Anca-Couce, Reaction mechanisms and multi-scale modelling of lignocellulosic biomass pyrolysis, Prog. Energy Combust. Sci. 53 (2016) 41–79, https://doi.org/10.1016/j.pecs.2015.10.002.

[5] N. Boonmee, J.G. Quintiere, Glowing ignition of wood: the onset of surface combustion, Proc. Combust. Inst. 30 (2005) 2303–2310, https://doi.org/10.1016/j.proci.2004.07.022.

[6] F. Richter, A. Atreya, P. Kotsovinos, G. Rein, The effect of chemical composition on the charring of wood across scales, Proc. Combust. Inst. 000 (2018) 1–9, https://doi.org/10.1016/j.proci.2018.06.080.

[7] A. Anca-Couce, N. Zobel, A. Berger, F. Behrendt, Smouldering of pine wood: kinetics and reaction heats, Combust. Flame 159 (2012) 1708–1719, https://doi.org/10.1016/j.combustflame.2011.11.015.

[8] G. Rein, C.W. Lautenberger, A.C. Fernandez-Pello, J.L. Torero, D.L. Urban, Application of genetic algorithms and thermogravimetry to determine the kinetics of polyurethane foam in smoldering combustion, Combust. Flame 146 (2006) 95–108, https://doi.org/10.1016/j.combustflame.2006.04.013.

[9] E. Ranzi, P.E.A. Debiagi, A. Frassoldati, Mathematical modeling of fast biomass pyrolysis and bio-oil formation. Note II: secondary gas-phase reactions and bio-oil formation, ACS Sustain. Chem. Eng. 5 (2017) 2882–2896, https://doi.org/10.1021/acssuschemeng.6b03098.

[10] P.E.A. Debiagi, C. Pecchi, G. Gentile, A. Frassoldati, A. Cuoci, T. Faravelli, E. Ranzi, Extractives extend the applicability of multistep kinetic scheme of biomass pyrolysis, Energy Fuels 29 (2015) 6544–6555, https://doi.org/10.1021/acs.energyfuels.5b01753.

[11] R. Emberley, T. Do, J. Yim, J.L. Torero, Critical heat flux and mass loss rate for extinction of flaming combustion of timber, Fire Saf. J. 1 (2017), https://doi.org/10.1016/j.firesaf.2017.03.008.

[12] P. Reszka, J.L. Torero, Fire behavior of timber and lignocellulose, Lignocellul. Fibers Wood Handb. John Wiley & Sons, Inc., Hoboken, NJ, USA, 2016, pp. 553–581, https://doi.org/10.1002/9781118773727.ch22.

[13] A.G.W. Bradbury, Y. Sakai, F. Shafizadeh, A kinetic model for pyrolysis of cellulose, J. Appl. Polym. Sci. 23 (1979) 3271–3280, https://doi.org/10.1002/app.1979.070231112.

[14] W.C. Park, A. Atreya, H.R. Baum, Determination of pyrolysis temperature for charring materials, Proc. Combust. Inst. 32 (2009) 2471–2479, https://doi.org/10.1016/j.proci.2008.06.060.

[15] M.J. Spearpoint, J.G. Quintiere, Predicting the burning of wood using an integral model, Combust. Flame 123 (2000) 308–325, https://doi.org/10.1016/S0010-2180(00)00162-0.

[16] R.B. Bates, A.F. Ghoniem, Modeling kinetics-transport interactions during biomass torrefaction: the effects of temperature, particle size, and moisture content, Fuel 137 (2014) 216–229, https://doi.org/10.1016/j.fuel.2014.07.047.

[17] Y. Ding, K. Kwon, S.I. Stoliarov, R.H. Kraemer, Development of a semi-global reaction mechanism for thermal decomposition of a polymer containing reactive flame retardant, 37th Int. Symp. Combust. 000 (2018) 1–9, https://doi.org/10.1016/j.proci.2018.05.073.

[18] D. Shen, L. Zhang, J. Xue, S. Guan, Q. Liu, R. Xiao, Thermal degradation of xylan-based hemicellulose under oxidative atmosphere, Carbohydr. Polym. 127 (2015) 363–371, https://doi.org/10.1016/j.carbpol.2015.03.067.

[19] D. Shen, J. Hu, R. Xiao, H. Zhang, S. Li, S. Gu, Online evolved gas analysis by thermogravimetric-mass Spectroscopy for thermal decomposition of biomass and its components under different atmospheres: part I. Lignin, Bioresour. Technol. 130 (2013) 449–456, https://doi.org/10.1016/j.biortech.2012.11.081.

[20] N. Bal, G. Rein, On the effect of inverse modelling and compensation effects in computational pyrolysis for fire scenarios, Fire Saf. J. 72 (2015) 68–76, https://doi.org/10.1016/j.firesaf.2015.02.012.

[21] A. Anca-Couce, I. Obernberger, Application of a detailed biomass pyrolysis kinetic scheme to hardwood and softwood torrefaction, Fuel 167 (2016) 158–167, https://doi.org/10.1016/j.fuel.2015.11.062.

[22] F. Richter, G. Rein, Pyrolysis kinetics and multi-objective inverse modelling of cellulose at the microscale, Fire Saf. J. 91 (2017) 191–199, https://doi.org/10.1016/j.firesaf.2017.03.082.

[23] M. Stenseng, a Jensen, K. Dam-Johansen, Investigation of biomass pyrolysis by thermogravimetric analysis and differential scanning calorimetry, J. Anal. Appl. Pyrolysis 58 (2001) 765–780, https://doi.org/10.1016/s0165-2370(00)00200-x.

[24] C. Branca, C. Di Blasi, Global interinsic kinetics of wood oxidation, Fuel 83 (2004) 81–87, https://doi.org/10.1016/S0016-2361(03)00220-5.

[25] G. Várhegyi, M.J. Antal, E. Jakab, P. Szabó, Kinetic modeling of biomass pyrolysis, J. Anal. Appl. Pyrolysis 42 (1997) 73–87, https://doi.org/10.1016/S0165-2370(96)00971-0.

[26] M.J. Antal, G. Varhegyi, E. Jakab, Cellulose pyrolysis kinetics: revisited, Ind. Eng. Chem. Res. 37 (1998) 1267–1275, https://doi.org/10.1021/ie970144v.

[27] G. Varhegyi, E. Jakab, M.J. Antal, Is the Broido-Shafizadeh model for cellulose pyrolysis true? Energy Fuels 8 (1994) 1345–1352, https://doi.org/10.1021/ef00048a025.

[28] T. Kashiwagi, H. Nambu, Global kinetic constants for thermal oxidative degradation of a cellulosic paper, Combust. Flame 88 (1992) 345–368, https://doi.org/10.1016/0010-2180(92)90039-R.

[29] R. Moriana, Y. Zhang, P. Mischnick, J. Li, M. Ek, Thermal degradation behavior and kinetic analysis of spruce glucomannan and its methylated derivatives, Carbohydr. Polym. 106 (2014) 60–70, https://doi.org/10.1016/j.carbpol.2014.01.086.

[30] S. Zhou, B. Pecha, M. van Kuppevelt, A.G. McDonald, M. Garcia-Perez, Slow and fast pyrolysis of Douglas-fir lignin: importance of liquid-intermediate formation on the distribution of products, Biomass Bioenergy 66 (2014) 398–409, https://doi.org/10.1016/j.biombioe.2014.03.064.

[31] C.E.L. Pasquali, H. Herrera, Pyrolysis of lignin and IR analysis of residues, Thermochim. Acta 293 (1997) 39–46, https://doi.org/10.1016/S0040-6031(97)00059-2.

[32] Y. Ding, O.A. Ezekoye, S. Lu, C. Wang, R. Zhou, Comparative pyrolysis behaviors and reaction mechanisms of hardwood and softwood, Energy Convers. Manage. 132 (2017) 102–109, https://doi.org/10.1016/j.enconman.2016.11.016.

[33] M.G. Grønli, G. Varhegyi, C. Di Blasi, G. Várhegyi, C. Di Blasi, Thermogravimetric analysis and devolatilization kinetics of wood, Ind. Eng. Chem. Res. 41 (2002) 4201–4208, https://doi.org/10.1021/ie0201157.

[34] M.J.C. Van Der Stelt, Chemistry and Reaction Kinetics of Biowaste Torrefaction, Eindhoven University of Technology, 2010, https://doi.org/10.6100/IR695294.

[35] Y. Su, Y. Luo, W. Wu, Y. Zhang, S. Zhao, Characteristics of pine wood oxidative pyrolysis: degradation behavior, carbon oxide production and heat properties, J. Anal. Appl. Pyrolysis 98 (2012) 137–143, https://doi.org/10.1016/j.jaap.2012.07.005.

[36] Q. Liu, S.R. Wang, M.X. Fang, M. Luo, K.F. Cen, W. Chow, Bench-scale studies on wood pyrolysis under different environments, AOFST 7 (2007).

[37] X. Huang, G. Rein, Thermochemical conversion of biomass in smouldering combustion across scales: the roles of heterogeneous kinetics, oxygen and transport phenomena, Bioresour. Technol. 207 (2016) 409–421, https://doi.org/10.1016/j.biortech.2016.01.027.

[38] J.A. Vrugt, B.A. Robinson, Improved evolutionary optimization from genetically adaptive multimethod search, Proc. Natl. Acad. Sci. 104 (2007) 708–711, https://doi.org/10.1073/pnas.0610471104.

[39] C. Di Blasi, M. Lanzetta, Intrinsic kinetics of isothermal xylan degradation in inert atmosphere, J. Anal. Appl. Pyrolysis 40–41 (1997) 287–303, https://doi.org/10.1016/S0165-2370(97)00028-4.

[40] J.J. Manyá, E. Velo, L. Puigjaner, J.J. Manya, E. Velo, L. Puigjaner, Kinetics of biomass pyrolysis: a reformulated three-parallel-Reactions model, Ind. Eng. Chem. Res. 42 (2003) 434–441, https://doi.org/10.1021/ie020218p.

[41] E. Ranzi, P.E.A. Debiagi, A. Frassoldati, Mathematical modeling of fast biomass pyrolysis and bio-oil formation. Note I: kinetic mechanism of biomass pyrolysis, ACS Sustain. Chem. Eng. 5 (2017) 2867–2881, https://doi.org/10.1021/acssuschemeng.6b03096.

[42] V. Mamleev, S. Bourbigot, J. Yvon, Kinetic analysis of the thermal decomposition of cellulose: the main step of mass loss, J. Anal. Appl. Pyrolysis 80 (2007) 151–165, https://doi.org/10.1016/j.jaap.2007.01.013.

[43] M. Frenklach, H. Wang, M.J. Rabinowitz, Optimization and analysis of large chemical kinetic mechanisms using the solution mapping method-combustion of methane, Prog. Energy Combust. Sci. 18 (1992) 47–73, https://doi.org/10.1016/0360-1285(92)90032-V.

[44] K. Raveendran, A. Ganesh, K.C. Khilar, Pyrolysis characteristics of biomass and biomass components, Fuel 75 (1996) 987–998.

[45] M. Frenklach, Transforming data into knowledge-Process Informatics for combustion chemistry, Proc. Combust. Inst. 31 (I) (2007) 125–140, https://doi.org/10.1016/j.proci.2006.08.121.

[46] R. Vinu, L.J. Broadbelt, A mechanistic model of fast pyrolysis of glucose-based carbohydrates to predict bio-oil composition, Energy Environ. Sci. (2012) 9808–9826, https://doi.org/10.1039/c2ee22784c.

[47] J. Cho, J.M. Davis, G.W. Huber, The intrinsic kinetics and heats of reactions for cellulose pyrolysis and char formation, ChemSusChem. 3 (2010) 1162–1165, https://doi.org/10.1002/cssc.201000119.

[48] J. Rath, M.G. Wolfinger, G. Steiner, G. Krammer, F. Barontini, V. Cozzani, Heat of wood pyrolysis, Fuel 82 (2003) 81–91, https://doi.org/10.1016/S0016-2361(02)00138-2.

[49] A. Leth-Espensen, P. Glarborg, P.A. Jensen, Predicting biomass char yield from high heating rate devolatilization using chemometrics, Energy Fuels 32 (2018) 9572–9580, https://doi.org/10.1021/acs.energyfuels.8b02073.

[50] X. Zhou, W. Li, R. Mabon, L.J. Broadbelt, A critical review on hemicellulose pyrolysis, Energy Technol. 08801 (2016) 1–29, https://doi.org/10.1002/ente.201600327.

[51] J. Cho, S. Chu, P.J. Dauenhauer, G.W. Huber, Kinetics and reaction chemistry for slow pyrolysis of enzymatic hydrolysis lignin and organosolv extracted lignin derived from maplewood, Green Chem. 14 (2012) 428–439, https://doi.org/10.1039/c1gc16222e.

[52] N. Bal, G. Rein, Relevant model complexity for non-charring polymer pyrolysis, Fire Saf. J. 61 (2013) 36–44, https://doi.org/10.1016/j.firesaf.2013.08.015.